Measurement of the $^1H(\gamma,\pi^0)$ cross section near threshold

J. C. Bergstrom, J. M. Vogt, R. Igarashi, K. J. Keeter, E. L. Hallin, G. A. Retzlaff, and D. M. Skopik
Saskatchewan Accelerator Laboratory, University of Saskatchewan, 107 North Road, Saskatoon, Saskatchewan, Canada S7N 5C6

E. C. Booth
Department of Physics, Boston University, 590 Commonwealth Avenue, Boston, Massachusetts 02215
(Received 20 November 1995)

The cross section for the reaction $^1H(\gamma,\pi^0)$ has been measured using tagged photons in the threshold region (144.7–169.3 MeV). The total cross section, augmented by angular distribution information, is used to deduce the *S*-wave multipole E_{0+}. Extrapolation to threshold yields $E_{0+}=(-1.32\pm0.05\pm0.06)\times10^{-3}/m_\pi$, in disagreement with earlier estimates. Suppression of E_{0+} near the π^+ threshold is confirmed, in approximate agreement with recent calculations.

PACS number(s): 25.20.Lj, 13.60.Le

The reaction $^1H(\gamma,\pi^0)$ has been measured within 25 MeV of threshold using tagged photons and a large acceptance π^0 spectrometer at the Saskatchewan Accelerator Laboratory (SAL). The total cross section and the pion angular distributions were independently investigated by configuring the π^0 spectrometer to the geometry most appropriate for the particular measurement. In this Rapid Communication we present a brief summary of these measurements. The principle objectives of this study were threefold: to clarify the energy dependence of the *S*-wave multipole E_{0+} at low energy; to determine E_{0+} at threshold; and finally, to resolve between conflicting claims for the strength of the *P*-wave multipole E_{1+} in the threshold region.

Let us briefly review the experimental and theoretical situations with respect to these objectives.

1. The $^1H(\gamma,\pi^0)$ measurements by Beck *et al.* [1] at Mainz revealed a pronounced energy dependence in the real part of E_{0+} that resisted explanation in terms of the usual models (Born terms, vector mesons, etc.). Although extracted at only five energies, the results suggested a strong suppression of E_{0+} near, and slightly above, the threshold for π^+ production. This behavior was also reflected in the Mainz total cross section. Unfortunately, the measurements were not extensive enough to indicate a possible "recovery" of ReE_{0+} with increasing energy.

2. Extrapolation of the Mainz total cross section to threshold [2,3] gives $E_{0+}=-2.1\pm0.2$ (in units of $10^{-3}/m_\pi$), in reasonable agreement with value $E_{0+}=-2.3$ predicted by the "classical" low energy theorem (LET) of de Baenst [4] and others. However, the low energy behavior of the *S*- and *P*-wave multipoles has recently been considered within the formalism of heavy baryon chiral perturbation theory (CHPT) by Bernard *et al.* [5], hereafter referred to as BKM. Allowing for isospin splitting of the pion masses, these calculations display the expected unitarity cusp in ReE_{0+} at π^+ threshold, and predict $E_{0+}=-1.16$ at π^0 threshold, substantially lower than both the experimental value and the LET prediction. A new feature in the CHPT formalism is a threshold contribution from the so-called triangle diagram, a nonanalytic term which seems contrary to the analyticity assumptions of the classical LET, and which acts to reduce the threshold amplitude. Now, it is generally accepted that E_{0+} is not an appropriate testing ground for CHPT in view of the apparent slow convergence of the chiral series. The main point, however, is that these new calculations have called into question the predictive power of the classical LET's, in which case the previous agreement between the LET and experiment must be considered as merely accidental. Such a surprising coincidence is clearly in need of independent experimental verification.

3. In their study of the low energy behavior of the *S*- and *P*-wave amplitudes within the CHPT formalism, BKM argue that, due to the rapid convergence of the chiral series (at least, to the order considered), the *P*-wave amplitudes should serve as a better testing ground for CHPT than E_{0+}. These authors present a set of *P*-wave LET's which can be rearranged as predictions for the quantities E_{1+} and $M_{1+}-M_{1-}$. These predictions were compared with experimental data in Ref. [6], and excellent agreement was observed for the combination $M_{1+}-M_{1-}$, but a marked discrepancy was noted concerning E_{1+}. Comparison was made at the level of the "reduced" multipole amplitudes which are assumed to be nearly constant at low energies, and which are defined by

$$e_{1+}=E_{1+}/qk, \quad \text{etc.} \tag{1}$$

Here q and k are, respectively, the pion and photon momenta in the c.m. frame, in units of the charged pion mass. The "experimental" result is [6]

$$e_{1+}(\text{expt})=-0.67\pm0.15, \tag{2}$$

while the CHPT prediction is [5]

$$e_{1+}(\text{CHPT})=-0.12 \tag{3}$$

in units of $10^{-3}/m_\pi$. An independent calculation within the more traditional effective Lagrangian formalism yields [7]

$$e_{1+}(\text{eff.Lag})=-0.02. \tag{4}$$

Thus, current theories seem to agree on a very small reduced E_{1+} amplitude near threshold, while the experimental value, Eq. (2), is nearly an order of magnitude larger. While an unambiguous confirmation of Eq. (2) will require polarization degrees of freedom, the pion angular distributions with unpolarized photons are quite sensitive to E_{1+} and permit a resolution of the extremes represented by Eqs. (2)–(4). Here

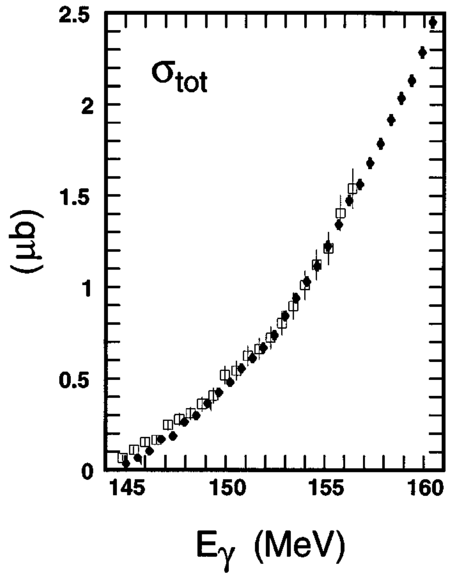

FIG. 1. Total cross section for ^{1}H(γ,π^0) below 160 MeV as a function of photon energy. The solid points represent the present results while the open squares are from Beck *et al.* [1].

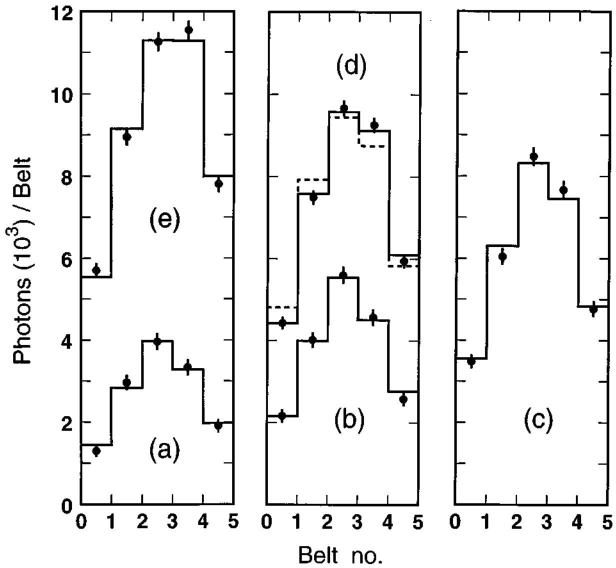

FIG. 2. Typical π^0-decay photon distributions along the five coaxial belts defining the Igloo detector. Belt No. 1 defines the forward direction. The incident photon energies for (a)–(e) are E_γ=152.2, 154.9, 160.7, 164.5, and 169.1 MeV, respectively. The solid histograms are fits using the global f_0 and p of Eqs. (14) and (15), with the ReE_{0+} as free parameters. The resulting ReE_{0+} are displayed in Fig. 4 (open circles).

we will rely upon theory to provide a rough constraint on the quantity $M_{1+}-M_{1-}$, although a precise prediction of this quantity is not essential for our analysis or conclusion.

The experiment was performed at SAL using the tagged photon facility [8] in conjunction with the π^0 spectrometer "Igloo" [9]. Bremsstrahlung was generated by an electron beam of energy 218.24 MeV within an energy spread of about 50 keV and a duty factor of 60–70 %, as provided by the pulse-stretcher ring EROS. The photon tagger was equipped with a 62-channel medium-resolution detector array that permitted a survey over an excitation region of 25 MeV using a single setting of the tagging spectrometer. Each channel of the array spanned about 500 keV in tagged photon energy.

The π^0 spectrometer Igloo consists of a rectangular box of 68 lead-glass detectors symmetrically arranged to define a hollow "cave" of dimensions 100×40×40 cm. In this configuration, used for total cross-section measurements, the geometric efficiency for π^0 detection near threshold is 83%. For pion angular distribution measurements, Igloo is split along a diagonal of the cave and each L-shaped arm is retracted about 42 cm. In this open configuration, information on pion angular distributions is obtained through two distinct methods, discussed in detail in [9]. In this Rapid Communication, information on the pion angular distribution will be retrieved using the "belt-hit" algorithm of [9]. The algorithm utilizes the π^0-decay photon distribution along the five coaxial "belts" defining Igloo, this distribution being a direct reflection of the pion angular distribution itself. The connection between the photon and pion distributions is made through Monte Carlo analysis, as discussed later. The absolute response of the spectrometer has been extensively modeled by Monte Carlo simulations, which have been verified by measurements of the ^{12}C(γ,π^0) reaction [9].

The target consisted of liquid hydrogen contained within a cylindrical Mylar cell 11 cm long and 6 cm in diameter. The spherical Mylar end caps were only 25 μm thick to minimize π^0 production from the cell. The effective target thickness was determined to an accuracy of $\pm$0.4% by measuring the forward pair production relative to a calibrated aluminum target, and utilizing the well-known atomic cross sections. Further experimental details will be described in a future paper.

Data were accumulated up to a maximum photon energy of 169.3 MeV. In Fig. 1 we show the total cross section below 160 MeV together with the Mainz data of Beck *et al.* [1]. Above π^+ threshold (151.44 MeV) excellent agreement exists between the two data sets, but they gradually diverge as one approaches π^0 threshold (144.67 MeV). In Fig. 2 we present a few of the photon belt-hit distributions accumulated when the Igloo detector is operated in the angular distribution (open) mode.

Close to threshold the photoproduction cross section is dominated by *S*- and *P*-wave pions, and with the exception of the *S*-wave amplitude E_{0+}, the respective amplitudes may be considered as real. In this scenario the ^{1}H(γ,π^0) cross section in the c.m. frame may be written

$$\frac{k}{q}\frac{d\sigma}{d\Omega}=a+b\,\cos\theta+c\,\sin^2\theta. \tag{5}$$

The coefficients in Eq. (5) are further defined by

$$\begin{aligned} a&=|E_{0+}|^2+P^2,\\ b&=2P\cdot\mathrm{Re}E_{0+},\\ c&=Q^2-P^2, \end{aligned} \tag{6}$$

where P and Q depend solely on the P-wave multipoles, i.e.,

$$P=3E_{1+}+M_{1+}-M_{1-} \tag{7}$$

while the more complicated structure of Q, not needed here, is given in [6].

Similarly, the total cross section is given by

$$\frac{k}{q}\,\sigma=4\pi(|E_{0+}|^2+\tfrac{1}{3}P^2+\tfrac{2}{3}Q^2), \tag{8}$$

or, in terms of the multipoles,

$$\frac{k}{q}\,\sigma=4\pi(|E_{0+}|^2+2M_{1+}^2+M_{1-}^2+6E_{1+}^2). \tag{9}$$

In order to facilitate a joint analysis of the (independently measured) total cross section and angular distributions, and to ensure continuity of the P-wave amplitudes with energy, we introduce a transformation of variables and employ the familiar low energy approximation for the P waves. We define the reduced P-wave amplitude f_0 through the multipole combination

$$2M_{1+}^2+M_{1-}^2+6E_{1+}^2=2f_0^2(qk)^2 \tag{10}$$

and the cross-section equation (9) becomes

$$\frac{k}{q}\,\sigma=4\pi\{|E_{0+}|^2+2f_0^2(qk)^2\}. \tag{11}$$

From Eqs. (8) and (11) we now eliminate Q^2 as a variable in favor of f_0:

$$Q^2=(3f_0^2-\tfrac{1}{2}p^2)\cdot(qk)^2, \tag{12}$$

where the reduced amplitude p is defined by

$$p=P/qk=(3E_{1+}+M_{1+}-M_{1-})/(qk). \tag{13}$$

The transformation is especially useful because the upper bound on f_0 is constrained by the experimental cross section through Eq. (11).

At this stage we are faced with four unknowns—the local values of ReE_{0+} and ImE_{0+} and the global reduced amplitudes f_0 and p. In order to make a statement about the real part of E_{0+} we need to make some assumption concerning ImE_{0+}. Between the π^0 and π^+ thresholds, ImE_{0+} is of course completely negligible. Above the π^+ threshold we rely on the calculation of Ref. [2], based on the elementary constraints of unitarity.

In principle, the pion angular distributions are sufficient for determining the S-wave multipole through Eqs. (5) and (6). However, the angular resolution of Igloo gradually deteriorates as one approaches π^0 threshold, so we will also employ Eq. (11) together with the measured total cross section. Specifically, we will deduce f_0 and p at selected energies using both the total cross section and the angular distributions as constraints. A global value of f_0 will then be established and used in Eq. (11) to extract $|E_{0+}|^2$ from $\sigma_{\rm tot}$ at all energies.

To determine f_0 and p we proceed as follows. First, we use Eq. (11) together with the experimental total cross section to deduce ReE_{0+} at selected energies, as a function of the free parameter f_0. The fact that $|E_{0+}|^2$ is positive definite sets an upper bound on f_0, specifically $f_0\leqslant 8.0$ in units of $10^{-3}/m_\pi$. A lower bound can also be roughly defined, $f_0\geqslant 7.7$, otherwise the resulting S-wave amplitudes would be totally incompatible with all previous determinations. Then, for a given local value of f_0 and its associated ReE_{0+}, we compare with the respective pion angular distribution, using Eqs. (12), (6), and (5). As noted, this comparison is done at the level of the photon "belt-hit" patterns through Monte Carlo simulations. For a given f_0 (and hence ReE_{0+}), the remaining parameter p is optimized. Finally, this is repeated over the bounded range of f_0 until both f_0 and p are optimized *at a given energy*. The selectivity of the analysis is illustrated by the example shown in Fig. 2(d). The dashed histogram derives from $f_0=8.00$ with ReE_{0+} constrained by $\sigma_{\rm tot}$ as described, while p has been optimized to yield the best fit to the pattern ($p\approx 10.0$). The solid histogram, on the other hand, corresponds to our final global parameters Eqs. (14) and (15) below.

It is important to note that the Monte Carlo simulations do not attempt to reproduce the absolute values of the differential cross section, but only the relative angular response, which depends on relative values of the coefficients in Eq. (5). In other words, the absolute detection efficiency of Igloo in the "open" mode is not a factor, greatly simplifying the analysis. The absolute values of the coefficients are calibrated by the total cross section measured with Igloo in the "closed" mode, where the detection efficiencies are well understood.

The weighted mean values of the reduced amplitudes f_0 and p determined by this procedure are

$$f_0=(7.90\pm 0.03)\times 10^{-3}/m_\pi \tag{14}$$

and

$$p=(9.2\pm 0.3)\times 10^{-3}/m_\pi. \tag{15}$$

Our value for f_0 compares nicely with the result deduced in a previous study, $f_0=7.90\pm 0.04$ [2], even though the present measurements extend 15 MeV further from threshold. Indeed, we detect no significant energy dependence in f_0, consistent with the assumption underlying Eq. (10). Also, p given by Eq. (15) is in reasonable agreement with the value derived from the reduced P-wave multipoles of Ref. [6], $p=8.8\pm 0.5$, but is somewhat larger than the value reported by Beck *et al.* [1], $p=8.3\pm 0.2$ (their M_1 is equivalent to our P). A mild increase in p is evident with decreasing energy, but since the errors on p become rather large near threshold, we must be content with the weighted mean over the entire energy domain.

With f_0 and p now fixed globally we may extract ReE_{0+} solely from the angular distributions, thus providing a consistency check against the ReE_{0+} to be derived from the total cross section. Thus, the solid histograms in Fig. 2 illustrate typical fits to the belt-hit patterns using Eqs. (14) and (15) but treating the ReE_{0+} as free parameters. Examples of the resulting ReE_{0+} are included in Fig. 4 (open circles) for later comparison. The angular analysis is not pursued below 152 MeV due to the rapid deterioration of the pion angular resolution near threshold.

The quantity $|E_{0+}|^2=[\mathrm{Re}E_{0+}]^2+[\mathrm{Im}E_{0+}]^2$, as extracted from the total cross section using Eqs. (11) and (14), is presented in Fig. 3. It displays a monotonic decrease in magnitude as the π^+ threshold is approached, followed by a roughly linear increase beyond. This linear behavior reflects the expected energy dependence of ImE_{0+} (which is propor-

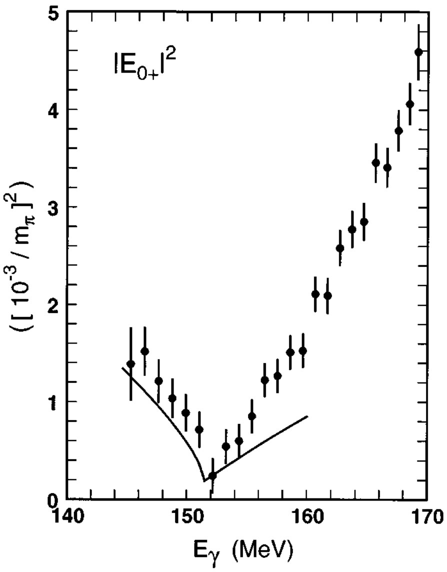

FIG. 3. The quantity $|E_{0+}|^2=[\mathrm{Re}E_{0+}]^2+[\mathrm{Im}E_{0+}]^2$ as deduced from the total cross section using Eq. (11) together with the result Eq. (14). The units are $10^{-6}/m_\pi^2$. These results have been rebinned relative to the original data of Fig. 1 by combining adjacent pairs of data points. The solid curve represents the CHPT prediction of Ref. [5]. For comparison, the classical LET prediction is $|E_{0+}|^2\approx 5.3$ at π^0 threshold, clearly inconsistent with experiment.

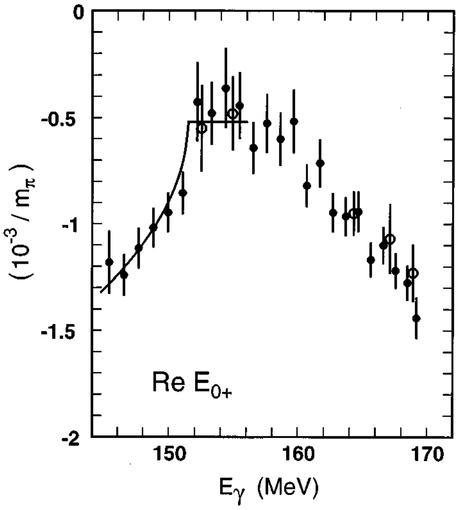

FIG. 4. The real part of E_{0+} in units of $10^{-3}/m_\pi$. The solid points, rebinned as in Fig. 3, follow from the analysis of the total cross section, while the open circles are derived from the angular distribution measurements. The curve illustrates Eq. (16) as evaluated with the threshold amplitudes Eqs. (17) and (18) and $\alpha=3.0\times10^{-3}/m_\pi^2$.

tional to q_{π^+}), together with a steady increase in the real component. Below π^+ threshold, the imaginary component is negligible and we observe $[\mathrm{Re}E_{0+}]^2$ directly.

The solid curve in Fig. 3 represents the CHPT prediction of BKM. The increasing disparity with experiment above the π^+ threshold is not unexpected since, as stressed in [5], the imaginary amplitude is less accurately calculated than the real amplitude. On the other hand, the CHPT description between the two thresholds is seen to be rather reasonable, if slightly low. In particular, the theory largely accounts for the suppression of E_{0+} near the π^+ threshold, and replicates the slope of $|E_{0+}|^2$ between the two thresholds. The level of agreement displayed in Fig. 3 is perhaps somewhat surprising considering the slow convergence of the chiral expansion at threshold, as emphasized by Bernard *et al.* However, from Fig. 3 it would appear that CHPT to order O(q^4) does indeed adequately describe E_{0+}, at least in the low energy region below π^+ threshold. While higher order terms individually may be far from negligible, their collective contribution must be relatively small.

Finally, the real component ReE_{0+} is displayed in Fig. 4. These results obtain from $|E_{0+}|^2$ by removing ImE_{0+} as calculated in [2]. Also shown in Fig. 4 are a few values of ReE_{0+} derived solely from the angular distribution measurements as previously described. The satisfactory agreement is an affirmation of the analysis procedure, since both sets of measurements must yield consistent amplitudes.

With respect to our introductory remarks we confirm the suppression of ReE_{0+} near and slightly above the π^+ threshold, although not to the extent previously reported. However, we now observe a gradual increase in the amplitude with increasing energy, a feature so far not adequately described by the CHPT calculations. An increase in ReE_{0+} with energy is anticipated if the present results are to extrapolate smoothly to the values deduced at higher energy, for example, in Ref. [10].

Let us consider now the threshold amplitude obtained by extrapolating the present results to the π^0 threshold. For this purpose we assume E_{0+} at low energy can be parametrized by the expression

$$E_{0+}=E_{0+}(\pi^+_{\mathrm{thr}})+i\alpha q_+ , \tag{16}$$

where $E_{0+}(\pi^+_{\mathrm{thr}})$ is the π^0 amplitude at the π^+ threshold, α is described below, and q_+ is the onshell π^+ momentum (in the π^+-neutron c.m. frame) as evaluated at the same E_γ. Below the π^+ threshold $q_+\rightarrow +i|q_+|$ and E_{0+} becomes real. The structure of Eq. (16) follows from unitarity and a similar form also arises in the CHPT treatment with isospin splitting [5]. The "constant" α is proportional to the $\pi^+n\rightarrow\pi^0p$ charge exchange amplitude, which must be extrapolated into the nonphysical domain below π^+ threshold. The CHPT calculations of BKM suggest that α remains relatively constant across the π^+ threshold.

The form of Eq. (16) implies that ReE_{0+} remains constant everywhere above π^+ threshold. Since Fig. 4 proves otherwise, especially above 160 MeV, we will confine ourselves to energies up to $E_\gamma^{\mathrm{max}}\leqslant 160$ MeV.

A least-squares analysis using Eq. (16) has been applied to both $|E_{0+}|^2$ and ReE_{0+} with similar results. At the π^0 and π^+ thresholds we find, in the canonical units,

$$E_{0+}(\pi^0_{\mathrm{thr}})=-1.32\pm0.05\pm0.06, \tag{17}$$

$$E_{0+}(\pi^+_{\mathrm{thr}})=-0.52\pm0.04\pm0.16, \tag{18}$$

where the first error is statistical and the second is associated with the various systematic uncertainties. The corresponding CHPT predictions are $E_{0+}(\pi^0_{\mathrm{thr}})=-1.16$ and $E_{0+}(\pi^+_{\mathrm{thr}})=-0.44$. The relative agreement between theory and experiment at the two thresholds quantifies the success of the CHPT formalism. This is especially evident when, with reference to Fig. 3, one realizes that the corresponding ''classical'' LET prediction $[\mathrm{Re}E_{0+}]^2 \approx 5.3$ is clearly incompatible with this experiment.

Consistent threshold results between $\mathrm{Re}E_{0+}$ and $|E_{0+}|^2$ are only possible when the values of α in Eq. (16), above and below π^+ threshold (α_+ and α_-, respectively), are allowed to differ. Specifically, we find $\alpha_+ = 3.8$ and $\alpha_- = 3.0$ in units of $10^{-3}/m_\pi^2$. The former agrees nicely with the value $\alpha_+ = 3.9$ as deduced from the model for $\mathrm{Im}E_{0+}$ presented in [2], and thus lends some credence to that model. A possible resolution of the unphysical discontinuity in α may reside in a continuation of the slope in $\mathrm{Re}E_{0+}$, evident in Fig. 4, into the region between the two thresholds. To explore this possibility we have modified Eq. (16) by the replacement $E_{0+}(\pi^+_{\mathrm{thr}}) \rightarrow \gamma + \beta q^4$ where q is the π^0 momentum and β, γ are constants. A reanalysis of $\mathrm{Re}E_{0+}$ yields a set of parameters that are independent of the cutoff E_γ^{max}, even when extended to the maximum of 169 MeV. [This situation does not obtain with a purely quadratic modification of Eq. (16).] We find $\alpha_- = 3.8$, now consistent with $\alpha_+ = 3.8$ as deduced solely from $|E_{0+}|^2$. The threshold amplitudes from this reanalysis are $E_{0+}(\pi^0_{\mathrm{thr}}) = -1.36 \pm 0.05$ and $E_{0+}(\pi^+_{\mathrm{thr}}) = -0.42 \pm 0.06$. Comparison with Eqs. (17) and (18) therefore provides a measure of the model dependence of our extrapolation procedure.

We can now address the second introductory item, the ''coincidence'' between the classical LET and experiment. The coincidence no longer exists. The earlier conclusion was based on an analysis of the Mainz total cross section. However, as we have noted, the present cross section below the π^+ threshold is smaller than the Mainz cross section, thus implying a smaller threshold amplitude than the latter data would suggest.

Upon completion of the present work we learned of a new threshold measurement at Mainz [11]. The authors report $E_{0+}(\pi^0_{\mathrm{thr}}) = -1.31 \pm 0.08$, with which our result, Eq. (17), is in excellent agreement.

We now turn to the P-wave amplitudes, focusing on the discrepancy between the $E2$ multipoles (E_{1+}) described earlier. In particular, we will demonstrate how the present measurements favor the previous ''experimental'' value, Eq. (2), over the theoretical predictions, Eqs. (3) and (4).

As noted earlier, the theoretical predictions for the combination $M_{1+} - M_{1-}$ near threshold are fairly reliable. For the present demonstration it is sufficient to adopt the mean value of the respective amplitudes of [5] and [7], giving

$$(M_{1+} - M_{1-})/qk = 11.0 \pm 0.4. \tag{19}$$

Inserting this estimate and our result for p [Eq. (15)] into Eq. (13) yields

$$e_{1+} = -0.60 \pm 0.23, \tag{20}$$

where the conservative error is based on a linear combination of the separate errors.

Another line of argument incorporates both p and f_0 and hinges on the reduced multipole m_{1-}. From the definitions of f_0 and p together with their numerical estimates [Eqs. (14) and (15)] we may deduce m_{1-} as a function of e_{1+}. Considering the two extremes as represented by theory ($e_{1+} \approx -0.07 \pm 0.05$) and Eq. (20), one finds $m_{1-} \approx -1.6 \pm 0.2$ and $m_{1-} \approx -3.6 \pm 1.0$, respectively. As a theoretical benchmark for m_{1-} we employ the value $m_{1-} = -3.45$ as evaluated by Benmerrouche [7] using the effective Lagrangian formalism, and which compares favorably with previous experimental estimates [6]. As judged against this benchmark, the value of m_{1-} deduced from Eq. (20) is acceptable and the alternative value is clearly excluded.

To summarize the present discussion, our results support the $E2$ amplitude given in Eq. (2), but not the theoretical estimates of Eq. (3) or Eq. (4). In other words, we confirm the discrepancy outlined in the Introduction. We therefore conclude that the current theoretical understanding of the $E2$ multipole in the threshold region is inadequate, which is puzzling since the same formalisms give acceptable descriptions of the magnetic dipole ($M1$) amplitudes. This conclusion is conditional that the threshold value of p does not rise substantially above the mean given by Eq. (15).

We thank Ulf-G. Meissner for communicating results to us prior to publication. This work was supported in part by the Natural Sciences and Engineering Research Council of Canada.

[1] R. Beck *et al.*, Phys. Rev. Lett. **65**, 1841 (1990).
[2] J. C. Bergstrom, Phys. Rev. C **44**, 1768 (1991).
[3] A. M. Bernstein and B. R. Holstein, Comments Nucl. Part. Phys. **20**, 197 (1991); D. Drechsel and L. Tiator, J. Phys. G **18**, 449 (1992).
[4] P. deBaenst, Nucl. Phys. **B24**, 633 (1970).
[5] V. Bernard, N. Kaiser, and Ulf-G. Meissner, Z. Phys. C (to be published).
[6] J. C. Bergstrom, Phys. Rev. C **52**, 1986 (1995).
[7] M. Benmerrouche (private communication).
[8] J. M. Vogt, R. E. Pywell, D. M. Skopik, E. L. Hallin, J. C. Bergstrom, and H. S. Caplan, Nucl. Instrum. Methods Phys. Res. Sect. A **324**, 198 (1993).
[9] J. M. Vogt, J. C. Bergstrom, R. Igarashi, and K. J. Keeter, Nucl. Instrum. Methods Phys. Res. Sect. A **366**, 100 (1995).
[10] F. A. Berends and D. L. Weaver, Nuc. Phys. **B30**, 575 (1971); W. Pfeil and D. Schwela, *ibid.* **B45**, 379 (1972).
[11] M. Fuchs *et al.*, Phys. Lett. B (to published).